Epidermal Growth Factor Triggers an Original, Caspase-independent Pituitary Cell Death with Heterogeneous Phenotype

Joanna Fombonne, Stéphanie Reix, Ramahefarizo Rasolonjanahary, Emmanuelle Danty, Sylvie Thirion, Geneviéve Laforge-Anglade, Olivier Bosler, Patrick Mehlen, Alain Enjalbert, Slavica Krantic

▶ **To cite this version:**

Joanna Fombonne, Stéphanie Reix, Ramahefarizo Rasolonjanahary, Emmanuelle Danty, Sylvie Thirion, et al.. Epidermal Growth Factor Triggers an Original, Caspase-independent Pituitary Cell Death with Heterogeneous Phenotype. Molecular Biology of the Cell, 2004, 15 (11), pp.4938-4948. 10.1091/mbc.e04-07-0601 . hal-04186854

HAL Id: hal-04186854
https://hal.inrae.fr/hal-04186854

Submitted on 24 Aug 2023

HAL is a multi-disciplinary open access archive for the deposit and dissemination of scientific research documents, whether they are published or not. The documents may come from teaching and research institutions in France or abroad, or from public or private research centers.

L'archive ouverte pluridisciplinaire **HAL**, est destinée au dépôt et à la diffusion de documents scientifiques de niveau recherche, publiés ou non, émanant des établissements d'enseignement et de recherche français ou étrangers, des laboratoires publics ou privés.

Molecular Biology of the Cell
Vol. 15, 4938–4948, November 2004

Epidermal Growth Factor Triggers an Original, Caspase-independent Pituitary Cell Death with Heterogeneous Phenotype

Joanna Fombonne,* Stéphanie Reix,* Ramahefarizo Rasolonjanahary,* Emmanuelle Danty,† Sylvie Thirion,* Geneviéve Laforge-Anglade,* Olivier Bosler,* Patrick Mehlen,† Alain Enjalbert,* and Slavica Krantic*‡

*Interactions Cellulaires Neuroendocriniennes, Unité Mixte de Recherche 6544, Centre National de Recherche Scientifique/Université de la Méditerranée, Institut Jean Roche, Faculté de Médecine Nord, 13916 Marseille, France; and †Apoptose/Différenciation, Centre de Génétique Moléculaire et Cellulaire, Label "La Ligue" Unité Mixte de Recherche 5534 Centre National de Recherche Scientifique/Université Claude Bernard, 69622 Villeurbanne, France

Submitted July 18, 2004; Accepted August 9, 2004
Monitoring Editor: Guido Guidotti

Programmed cell death (PCD) is physiologically involved in the regulation of cell division and differentiation. It encompasses caspase-dependent mitochondrial and nonmitochondrial pathways. Additional caspase-independent pathways have been characterized in mitochondrial PCDs but remain hypothetical in nonmitochondrial PCDs. Epidermal growth factor (EGF) has been shown to inhibit division of pituitary somato-lactotrope cells occurring in parallel with EGF-mediated differentiation of these precursors into lactotrope cells. We show here that in somato-lactotrope pituitary cell line GH4C1, EGF triggers a PCD characterized by an apoptosis-like DNA fragmentation, insensitivity to broad-range caspase inhibitors, and absence of either cytochrome *c* or apoptosis-inducing factor release from mitochondria. Dying cells display loose chromatin clustering and numerous cytoplasmic vacuoles, a fraction of which are autophagic, thus conferring a heterogeneous phenotype to this PCD. Moreover, overexpression of cell death inhibitor Bcl-2 prevented not only the EGF-induced PCD but also its prodifferentiation effects, thus pointing to a mechanistic relationship existing between these two phenomena. Overall, the characterized differentiation-linked cell death represents an original form of caspase-independent PCD. The mechanisms underlying this PCD involve combinatorial engagement of discrete death effectors leading to a heterogeneous death phenotype that might be evolutionary related to PCD seen during the differentiation of some unicellular organisms.

INTRODUCTION

Programmed cell death (PCD) is physiologically involved in the control of proliferation/differentiation balance both in the course of development (e.g., organogenesis in mammals) and during the optimization of adult cell/tissue functions (e.g., thymic maturation of T lymphocytes). More recently, PCD has been associated with some pathological processes such as cancer and neurodegeneration. There is currently no consensus on either definition or classification of PCD (Sloviter, 2002; Golstein *et al.*, 2003). The "programmed" character occurs as a hallmark of PCD, but it refers to different aspects of the phenomenon, i.e., to the programmed occurrence of PCD in the course of development (in developmental PCD) or to the programmed succession of morphological and biochemical events (in nondevelopmental PCDs). However, the term programmed is also considered in the sense of "regulated," leading to a broad classification of PCD into apoptosis, necrosis, and autophagy (Golstein *et al.*, 2003). One of the more restraining classifications is based on a particular criterion of the nuclear morphology and divides PCDs into classical apoptosis, apoptosis-like PCD, and necrosis-like PCD characterized by "crescent-like" (type 2), lumpy (type 1), or absence of chromatin condensation, respectively (Jaattela and Tschopp, 2003).

Classical apoptosis is the best known phenotypic expression of PCD. It is related to a series of stereotypic morphological and biochemical alterations resulting from the activation of cystein-dependent aspartate-directed proteases called caspases. The canonical pathway of caspase activation is achieved through mitochondrial route via cytochrome *c* release involved in "executive" caspase-3 activation (Budihardjo *et al.*, 1999). This pathway is associated with caspase-activated DNase activation, leading to the typical internucleosomal DNA fragmentation. More recently, another caspase-independent mitochondrial pathway has been characterized. This pathway is mediated through apoptosis-inducing factor (AIF) release from the intramembrane mitochondrial space and its subsequent translocation to the nucleus. AIF triggers DNA fragmentation into the large fragments corresponding to type 1 chromatin condensation characteristic of apoptosis-like PCD (Jaattela and Tschopp, 2003).

Nonmitochondrial caspase-dependent PCDs have also been described. The most studied among these pathways is

Article published online ahead of print. Mol. Biol. Cell 10.1091/mbc.E04–07–0601. Article and publication date are available at www.molbiolcell.org/cgi/doi/10.1091/mbc.E04–07–0601.

‡ Corresponding author. E-mail address: krantic.s@jean-roche.univ-mrs.fr.

© 2004 by The American Society for Cell Biology

death receptor-mediated classical apoptosis (Nagata, 1997). The existence of the additional nonmitochondrial, caspase-dependent pathways associated with endoplasmic reticulum stress- (Rao *et al.*, 2001) and dependence receptor (Forcet *et al.*, 2001)-induced apoptosis have been reported. By analogy to the mitochondrial caspase-independent PCDs, it has been proposed that nonmitochondrial, caspase-independent PCDs should exist (Borner, 2003), but they have not been discovered yet.

Epidermal growth factor (EGF) is one among the plethora of extracellular signals regulating the balance between cell division, differentiation, and death. These biological actions of EGF involve the high-affinity plasma membrane receptor (epidermal growth factor receptor [EGFR]/HER1/ErbB-1) and multiple downstream signaling cascades as extracellular signal-regulated kinase (ERK) and Janus kinase pathways (Bogdan and Klambt, 2001). EGF has the capacity to trigger cell proliferation (Partanen, 1990; Weiss *et al.*, 1996) and to rescue cells from apoptosis (Kanasaki *et al.*, 2000; Leu *et al.*, 2000), but it is also able to induce apoptosis (Danielsen and Maihle, 2002). Moreover, prodifferentiation effects of EGF have been documented in some cellular contexts. For instance, EGF triggers an increase of prolactine (PRL) and decrease of growth hormone (GH) secretion in somato-lactotrope pituitary cells in vitro (Johnson *et al.*, 1980). These alterations are reminiscent of what is observed upon EGF addition to primary cultures of neonatal pituitary cells (Felix *et al.*, 1995). Based on these data and on the histological detection of the EGF ligand/EGFR system in neonatal pituitaries of several species, it has been postulated that EGF promotes the differentiation of lactotropes from somato-lactotrope precursors (Felix *et al.*, 1995).

Prodifferentiation effects of EGF in somato-lactotrope pituitary cells are associated with the inhibition of cell division (Schonbrunn *et al.*, 1980) resulting from the block of G1/S phase transition in the cell cycle (Ramsdell, 1991). However, a possible contribution of the EGF-induced PCD to the observed decrease of somato-lactotrope cell number has not been studied so far. In the present study, we show that EGF effects on somato-lactotrope cell line involve an unusual type of caspase-independent PCD.

MATERIALS AND METHODS

Cell Culture, Hormone Assays, and Transfections

Rat somato-lactotrope GH4C1 cell line containing undetectable lactotrope cells (Kineman and Frawley, 1994) and pure lactotrope MMQ cells (Kineman and Frawley, 1994) were obtained from American Type Culture Collection (Rockville, MD). They were grown in Ham's F-10 (for GH4C1) or RPMI 1640 medium (for MMQ) supplemented with 10% horse serum and 2.5% (for GH4C1) or 5% (for MMQ) fetal calf serum. LβT2 gonadotrope cell line was obtained from Drs. P. Mellon (University of California, San Diego, San Diego, CA) and D. Weiner (University of California, San Francisco, San Francisco, CA). This cell line was grown in DMEM supplemented with 10% fetal bovine serum.

For hormone assays, cells were cultured in the presence of 1 nM EGF (Sigma-Aldrich, St. Louis, MO) concentration based on the previous reports by using pituitary (Birman *et al.*, 1987) cells, including GH4C1 cell line (Aanestad *et al.*, 1993). Nerve growth factor (NGF) (Sigma-Aldrich) was chosen as a negative control for EGF actions because these two growth factors use partly overlapping transduction pathways but induce morphologically and biochemically distinct cellular responses both in nonrelated (Huff and Guroff, 1981) and somato-lactotrope (Yoshinaga *et al.*, 1998) cell lines.

EGF or NGF was added to the cell cultures for 2 d. This time of treatment was chosen because it permits to measure a significant increase in PRL secretion (Felix *et al.*, 1995) without the medium replenishment. At the end of the treatment period, the medium was removed and replaced by fresh, serum-free medium. The accumulation of secreted PRL and GH in the medium was then measured over a 1-h period by subsequent standard GH- or PRL-RIAs (Epelbaum *et al.*, 1987).

The constructs used for cell transfection were obtained from P. Friesen (University of Wisconsin, Madison, WI) for pBabe-p35 or after the insertion of the cloned 1855-base pair cDNA fragment of Bcl-2 into pcDNA-3.1 vector (Hockenbery *et al.*, 1993). The transient GH4C1 cell transfection was performed by using TransFast reagent (Promega, Madison, WI).

Quantification of Cell Death

Dead cell number was assessed by trypan blue exclusion. At the end of the treatment periods, floating cells were collected and added to the cells detached from the well bottom by trypsinization. After centrifugation, cell pellets were resuspended in phosphate-buffered saline (PBS) to which trypan blue solution was added in a final concentration of 0.04%. Both total and dead cell numbers were determined by four independent hemocytometer counts in each experiment. The number of dead cells is expressed as a percentage of total cell number at the time of the treatment arrest.

Western Blot Conditions

Extracted proteins (30 μg/lane) were separated by SDS-PAGE, immobilized on nitrocellulose membrane by electrotransfer, and first blotted with either rabbit anti-phospho:(Thr202/Tyr204) p42/p44 ERK, (Thr183/Tyr185) SAPK/JNK, or (Thr180/Tyr182) p38 kinase antibodies (Cell Signaling Technology, Beverly, MA). After detection of the phosphorylated kinase isoforms by chemoluminescence (PerkinElmer Life and Analytical Sciences, Boston, MA), the bound antibodies were stripped off and the membranes were reblotted with either rabbit:anti-p42/p44 ERK, anti-SAPK/JNK, or anti-p38 kinase antibodies (Cell Signaling Technology). All primary antibodies were used in a 1:1000 dilution. The secondary, goat-anti-rabbit IgG antibody (Jackson Immunoresearch Laboratories, West Grove, PA) was used in a 1:10,000 dilution.

For caspase-3 detection, rabbit anticaspase-3 antibody (Santa Cruz Biotechnology, Santa Cruz, CA) was used at 1:800 dilution. The positive reaction was revealed by using goat anti-rabbit IgG antibody (Vector Laboratories, Burlingame, CA) in a 1:5000 dilution.

Assessment of Apoptosis by DNA Fragmentation, Caspase-3 Activity Assay, and Fluorescence-activated Cell Sorting (FACS) Analysis

DNA was extracted from both floating and adherent cells with phenol: chloroform:isoamyl alcohol (25:24:1) and precipitated from the aqueous phase with acetate:alcohol (0.5 volume of 7.5 M sodium acetate, 2 volumes of ethanol 100%).

Internucleosomal DNA fragmentation was detected by using ApoAlert LM-PCR ladder assay kit (BD Biosciences Clontech, Palo Alto, CA) and ApoDNA1 kit (Interchim, Montlucon, France). Caspase-3 activity was determined in the whole cell population (both floating and adhering cells) by measurement of Ac-DEVD-AFC substrate conversion with ApoAlert caspase-3 assay (BD Biosciences Clontech). The enzyme activity is expressed as a ratio of the activity measured for each sample over that measured at time 0.

For FACS analysis, control and EGF-treated cells were stained by propidium iodide (Sigma-Aldrich). Fluorescence resulting from the excitation with an Ar-laser was measured on 10,000 cells per condition using a FACScalibur flow cytometer (BD Biosciences, San Jose, CA). Electronic gates were set for viable cells with 2n (G1 phase), 4n (G2/M phase), and less than 2n ("sub"-G1 dying cells). Data were analyzed by Cell Quest software from BD Biosciences.

Immunocytochemistry and Confocal Microscopy

After permeabilization (0.1% Triton X-100; 5 min), cells were incubated overnight at 4°C with mouse anti-AIF (E-1; Santa Cruz Biotechnology) or with mouse anti-cytochrome *c* (BD Biosciences PharMingen, San Diego, CA), diluted at 1:100 in PBS supplemented with 0.5% bovine serum albumin. The immunostaining was visualized using an Alexa 488-conjugated goat anti-mouse IgG antibody (Molecular Probes, Eugene, OR) diluted in PBS containing 10% normal goat serum.

To assess the localization of mitochondria, cells were loaded with 200 nM MitoTracker CMXRos red dye (Molecular Probes) >40 min at 37°C before fixation. Confocal image acquisition was performed on a Leica TCS SP2 laser scanning microscope by using the 488-nm band of an Ar-laser and the 543-nm band of a He/Ne-laser for excitation of Alexa 488 and MitoTracker CMXRos, respectively. Image editing was performed using Adobe Photoshop.

Transmission Electron Microscopy

EGF-treated and control cells were fixed for 15 min at 4°C with a mixture of 2% paraformaldehyde and 2% glutaraldehyde in 0.1 M phosphate buffer (pH 7.4) containing 5% sucrose. The cells were washed and postfixed in 1% osmium tetroxide in 0.1 M phosphate buffer for 30 min at room temperature. Pellets obtained by centrifugation were then dehydrated in graded ethanols and embedded in Epon 812. Silver-gold ultrathin sections were collected on single-slot Formvar-coated grids and examined with a CM10 Philips electron microscope after staining with diluted lead citrate.

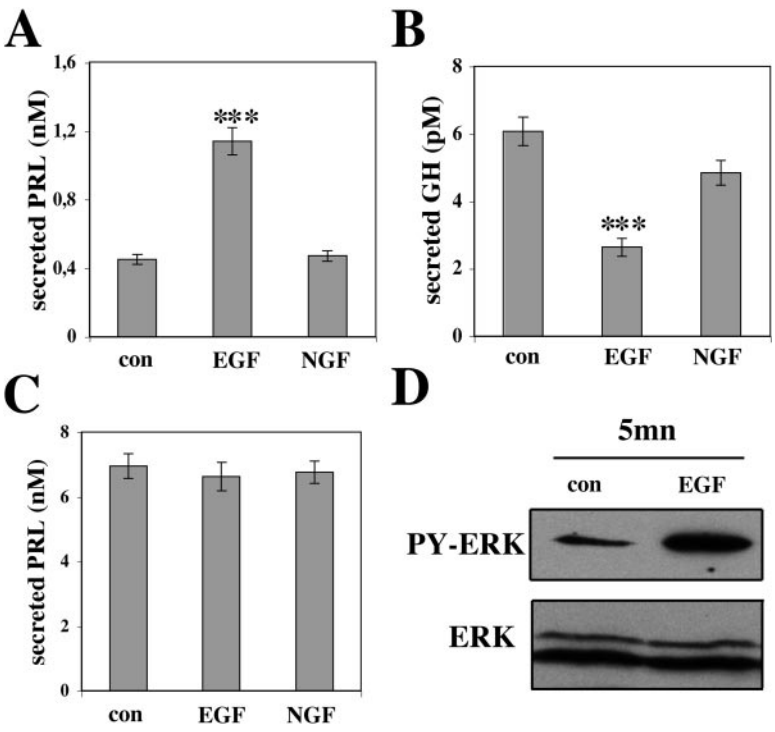

Figure 1. EGF triggers phenotype alterations in somato-lactotrope (GH4C1) but not in lactotrope (MMQ) pituitary cells. Growth factor effects on PRL (A and C) and GH (B) secretion in GH4C1 (A and B) and MMQ (C) cells. ***$p < 0.001$ for EGF-treated versus control (con) cells in A and B. (D) EGF-mediated ERK activation in MMQ cells. EGF triggers a rapid (i.e., 5 min after addition) tyrosine phosphorylation of ERK (PY-ERK) without altering the total ERK protein expression (ERK).

Data Analysis

If not otherwise specified, data are presented as the mean ± SEM of triplicate determinations performed in at least three independent experiments carried out with different cell preparations or cell cultures. Statistical significance was determined by analysis of variance by using PRISM software computer program. Post hoc comparisons between treatment group means were made with the Bonferroni test for multiple comparisons.

RESULTS

EGF-induced Alteration of Cell Phenotype Is Specific for Somato-Lactotrope Cells

To assess whether the previously reported EGF actions on hormone secretion of pituitary cells depend on their differentiation context, we studied in parallel the growth factor capacity to alter PRL and GH secretion by somato-lactotrope GH4C1 and lactotrope MMQ cells. As expected, after 48 h of treatment with EGF, GH4C1 cells secreted 3 times more PRL than control cells (Figure 1A). In contrast, EGF decreased GH secretion in treated cells to one-half of that seen in control cells (Figure 1B). The incubation of these cells over the same time period with NGF, used as a negative control, had no significant effect on either PRL (Figure 1A) or GH (Figure 1B) secretions.

Treatment of MMQ cells with either of two growth factors had no significant effect on PRL secretion (Figure 1C). Consistent with their pure lactotrope phenotype, GH secretion was undetectable in control MMQ cells and neither EGF nor NGF treatments were able to induce it (Rasolonjanahary and Krantic, unpublished data). To exclude a possibility that the absence of EGF actions on hormone secretion comes from the lack of the functional EGFR expression by MMQ cells, we studied the activation of the downstream ERK kinase (Bogdan and Klambt, 2001) by assessing its tyrosine phosphorylation. Our data show that EGF treatment for 5 min was sufficient to trigger ERK's tyrosine phosphorylation (Figure 1D), thus pointing to the presence of functional EGFR in MMQ cells.

The observed phenotypic alterations were accompanied with a dramatic, EGF-specific (i.e., NGF had no effect) decrease in the cell number of GH4C1 but not MMQ cells. The specificity of EGF effects on GH4C1 cells was attested by the fact that a selective inhibitor of EGFR tyrosine-kinase, PKI166 (Novartis AG, Basel, Switzerland) (Peles and Yarden, 1993; Mellinghoff *et al.*, 2002) could inhibit both a decrease in the cell number and increase in PRL secretion induced by EGF (Rasolonjanahary and Krantic, unpublished data).

Further experiments were therefore focused on the specific, EGF-induced decrease in GH4C1 cell number accompanying the alteration of their phenotype.

EGF-mediated Decrease in Cell Number Is Related to Concomitant Inhibition of Cell Division and Induction of Cell Death

We next asked whether the reported decrease in GH4C1 cell number could be attributed exclusively to the previously suggested cytostatic actions of EGF (Ramsdell, 1991) or whether it could also result from EGF-induced cell death. The presence of EGF induced a redistribution of cells in different phases of the cell cycle (Figure 2A). Thus, in EGF-treated cells, the number of cells in G2/M phase was reduced to at least one-half of that seen in control cells (Figure 2A). Interestingly, the number of cells containing less than a normal 2n DNA complement (characteristic of dying cells) was greater in EGF-treated than in control cells (Figure 2A, sub-G1).

A series of experiments were then designed to determine whether EGF triggers a PCD by apoptosis. Characteristic DNA-ladders could be revealed in DNA extracts from EGF-treated cells by ApoAlert LM-PCR ladder assay (Figure 2B, lanes 3 and 4). This ladder was similar to that seen in thymic DNA extracts used as a positive control (Figure 2B, lane 5). In contrast, no internucleosomal DNA fragmentation was observed in control cells (Figure 2B, lanes 1 and 2).

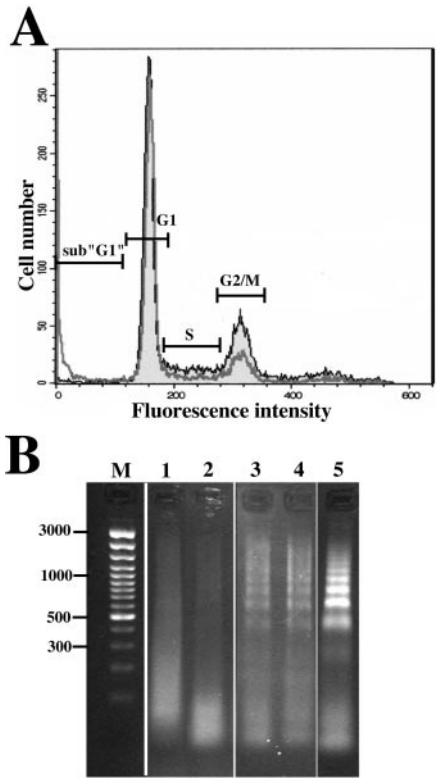

Figure 2. EGF triggers DNA fragmentation in GH4C1 cells. (A) Cell cycle distribution of GH4C1 cells incubated with 1 nM EGF (gray line) for 48 h or left untreated to serve as a control (black line). Shown is one overlay (EGF treated vs. control) of representative histograms from one of three independent FACS experiments in which similar results were obtained. (B) DNA fragmentation in GH4C1 cells treated for 48 h with 1 nM EGF (lanes 3 and 4 for samples obtained in two different cultures). Control cells (lanes 1 and 2) were negative in ApoAlert LM-PCR ladder assay, whereas thymic DNA (lane 5), used as a positive control, showed a characteristic DNA-laddering pattern. The size of DNA fragments (in base pairs) is given by the lane M.

Together, these data suggested that both diminished engagement in cell division and induction of PCD contribute to the observed EGF actions on GH4C1 cell number.

Intracellular Signaling Underlying EGF Actions on PRL Secretion and Cell Death

Given the common involvement of ERK pathway in EGF actions on other cell types (Bogdan and Klambt, 2001), we sought to determine whether the inhibition of ERK activation by U0126, a specific inhibitor of its upstream kinase mitogen-activated protein kinase kinase 1, might block the observed EGF actions on GH4C1 cells. As expected the EGF-dependent ERK activation, assessed by monitoring the critical tyrosine residue phosphorylation, was rapid (it was detected 5 min after EGF addition) and persistent up to the longest (30-min) time period studied (Figure 3A). The addition of 10 μM U0126 (Liu *et al.*, 2002b) markedly diminished this phosphorylation (lane EGF+U vs. lane EGF for 30-min time point in Figure 3A). U0126 also blocked the basal ERK phosphorylation (U vs. Con in Figure 3A).

In the same experimental conditions, U0126 blocked the EGF actions on the increase of PRL secretion (Figure 3B), but it was completely inefficient in preventing EGF-induced PCD (Figure 3C), thus suggesting that the EGF actions on cell death involve a different signaling pathway. Involvement of the other members of the same kinase family such as stress-activated protein kinase (SAPK)/c-Jun NH_2-terminal kinase (JNK) and p38 seems unlikely because EGF was not able to trigger any activation of these kinases as monitored by the assessment of the relevant tyrosine residue phosphorylation (Figure 3, D and E, respectively). This was in contrast with the observed gonadotropin release hormone (GnRH)-elicited tyrosine phosphorylation of SAPK/JNK and p38 (Figure 3, D and E, respectively) in LβT2 cells used as a positive control (Liu *et al.*, 2002a).

Therefore, EGF actions on both PRL secretion and cell death are mediated by functional EGFRs but only the former involves ERK pathway.

EGF-induced PCD Is Caspase Independent

To assess whether EGF-induced cell death involves the activation of the classical apoptotic pathway, we studied the enzymatic activation of caspase-3. In contrast to a classical apoptotic trigger staurosporine (5 μM), EGF was not able to induce the activation of this enzyme at any time point tested (Figure 4A vs. B). As expected for caspase-dependent apoptosis, 20 μM (Forcet *et al.*, 2001) Z-Val-Ala-Asp(*O*-methyl)-fluoromethylketone (Z-VAD.fmk; Bachem, Bubendorf, Switzerland) entirely prevented the enzyme activation by staurosporine (Figure 4A).

To further demonstrate the absence of any caspase-3 activation in EGF-treated cells, we performed a Western blot by using an antibody recognizing both immature procaspase-3 and its mature subunit. Indeed, a mature fragment of 17 kDa is generated from 32-kDa procaspase-3 precursor in the course of the proteolitical activation of this enzyme. Although we were able to detect the 17-kDa fragment in staurosporine-treated cells (5 μM; 24 h), the proteolytic cleavage of 32-kDa precursor was never observed in EGF-treated cells (Fombonne and Reix, unpublished data).

Moreover, Z-VAD.fmk was completely inefficient in blocking the increase in the number of dead cells induced by EGF after either 24 or 48 h of treatment (Figure 4C). The inefficiency of Z-VAD.fmk to prevent EGF-induced cell death was not due to the use of a suboptimal concentration because in the same experimental conditions, it completely prevented the rapid induction of cell death by staurosporine (Figure 4D).

To further confirm the absence of caspase involvement in EGF-induced cell death, we tested the capacity of additional caspase inhibitors on EGF-induced GH4C1 cell death. Neither 50 μM (Sperandio *et al.*, 2000) BOC-ASP(OMe).fmk (BOC.fmk; MP Biomedicals, Irvine, CA) nor transient transfection with pBabe-p35 could prevent the EGF-mediated increase in dead cell number (Figure 4, E and F, respectively). By contrast, staurosporine-induced cell death was efficiently blocked by these caspase inhibitors in both assays (Figure 4, E and F).

It is currently believed that in the classical caspase-dependent apoptosis pathway, only nuclear events (e.g., DNA fragmentation) are fully dependent on caspase activation (and thus blockable by the broad-range caspase inhibitors), whereas cytoplasmic hallmarks of apoptosis as well as cell death itself are not (Borner and Monney, 1999). To assess the caspase dependence of EGF-elicited DNA laddering, we performed an analysis of DNA fragmentation in GH4C1 cells treated with either EGF alone or in combination with caspase inhibitors. Our data show that neither Z-VAD.fmk nor BOC.fmk could prevent EGF-induced DNA fragmentation (Figure 4G).

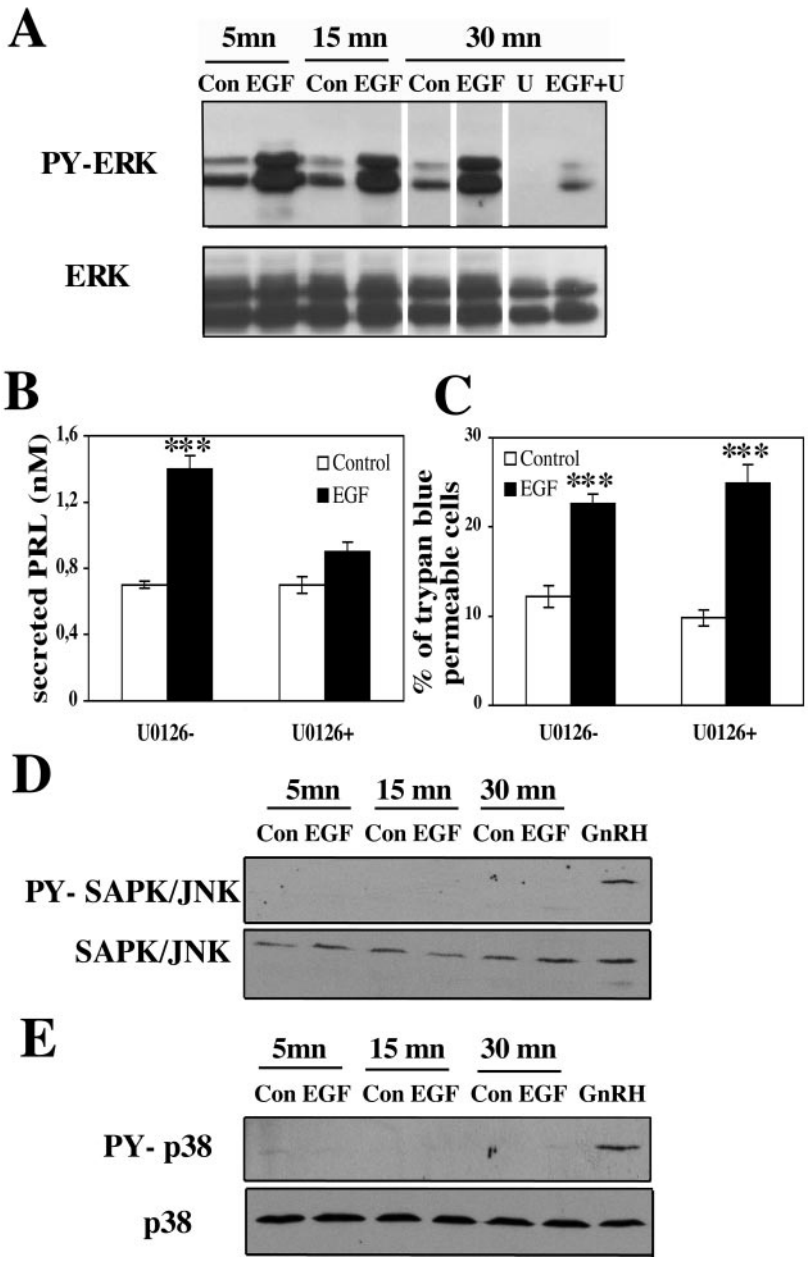

Figure 3. EGF actions on GH4C1 cells involve specific intracellular signaling. (A) EGF triggers tyrosine phosphorylation of ERK isoforms (PY-ERK) without alteration of the total ERK protein expression (ERK). Soluble protein extracts were obtained from: control (Con), 1 nM EGF-treated, 1 nM EGF plus 10 μM U0126 (EGF+U)-treated and control cells incubated with 10 μM U0126 (U). (B and C) Cells cultured for 48 h in the presence of EGF or left untreated (Control) were incubated in the absence (U0126-) or in the presence (U0126+) of the inhibitor of ERK activation. PRL secretion (B) and dead cell number (C) were assessed as described. ***$p < 0.001$ for EGF-treated vs. control groups in B and C. (D) GH4C1 cells (first six lanes) were left untreated (Con) or treated with EGF for the indicated time periods. LβT2 cells (last line) were treated with 0.1 μM GnRH (GnRH) for 30 min (Liu *et al.*, 2002a) to serve as a positive control. Soluble protein extracts were analyzed by SDS-PAGE and immunoblotted for either phospho-tyrosine SAPK/JNK (PY-SAPK/JNK) or total SAPK/JNK detection. (E) GH4C1 cells (first six lanes) were left untreated (Con) or treated with EGF for the indicated time periods. LβT2 cells (last line) were treated with 0.1 μM GnRH (GnRH) for 10 min (Liu *et al.*, 2002a) to serve as a positive control. Soluble protein extracts were analyzed by SDS-PAGE and immunoblotted with antibodies directed against either phospho-tyrosine p38 (PY-p38) or total p38.

Taken together, these data suggested a caspase independence of EGF-induced PCD.

EGF-induced PCD Is Independent of Classical Apoptosis-associated Mitochondrial Effectors

To determine the putative involvement of mitochondria-dependent pathways in EGF-induced PCD, we examined the mitochondrial membrane potential ($\Delta\varphi_m$) by using the potential-sensitive dye MitoTracker CMXRos. A collapse of $\Delta\varphi_m$ was observed in a fraction of EGF-treated cells, as attested by the decrease of red fluorescence (Figure 5A).

Although there is controversy regarding the meaning of the loss of $\Delta\varphi_m$ during PCD (whether it is a cause or a consequence of outer membrane permeabilization), the association of $\Delta\varphi_m$ impairment with cytochrome *c* and AIF release from mitochondria during PCD has been reported previously (Arnoult *et al.*, 2003). We therefore assessed the subcellular distribution of cytochrome *c* and AIF during EGF-induced PCD. Our data indicated that in the basal state cytochrome *c* was confined to mitochondria, as shown by the perinuclear, punctate staining pattern and its colocalization with MitoTracker CMXRos (Figure 5B). EGF treatment at both time points studied (3 and 24 h) was inefficient in triggering cytochrome *c* release from mitochondria to cytoplasm. However, in this regard two different cell subpopulations were seen. In one of them, cytochrome *c* and MitoTracker CMXRos staining colocalized as in controls whereas in the other cytochrome *c* staining remained punctuate despite the loss of MitoTracker CMXRos staining. This was in contrast to cytochrome *c* translocation seen in a fraction of cells treated by staurosporine (Figure 5B).

Immunofluorescence detection of AIF yielded a punctate cytoplasmic staining, typical for a mitochondrial localization. Accordingly, double-staining experiments allowing for

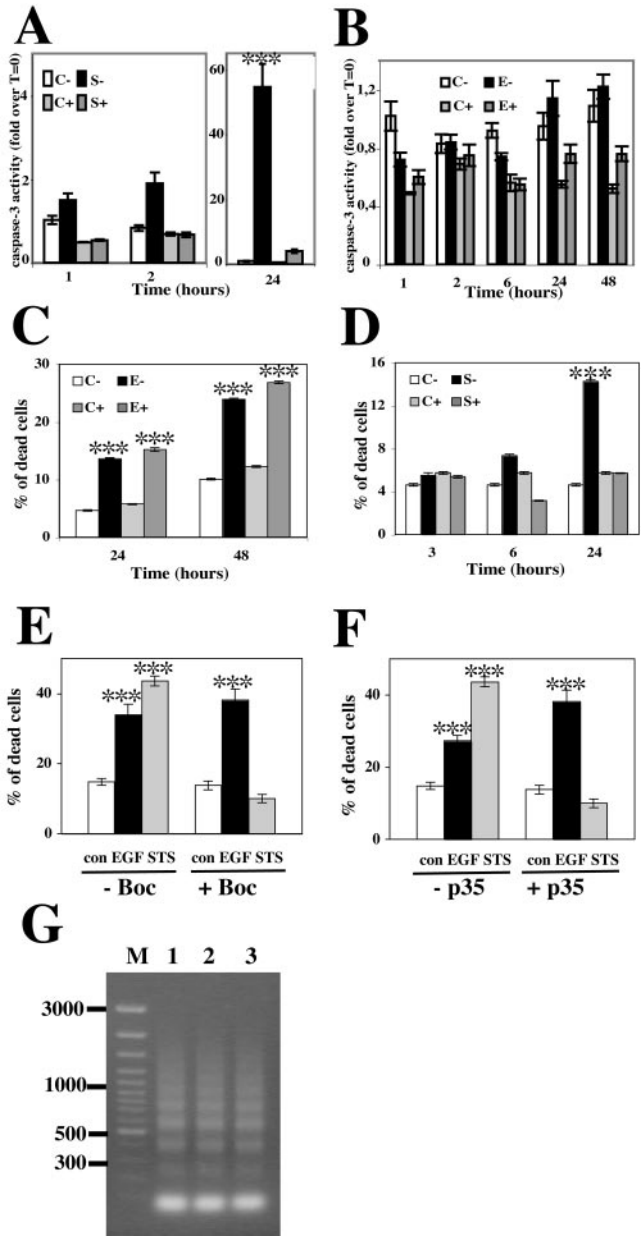

Figure 4. EGF-induced PCD in GH4C1 cells is not associated to caspase activation. (A and B) Caspase-3 activity measurement by ApoAlert caspase-3 assay in 5 μM staurosporine- (S), control (C), and 1 nM EGF (E)-treated cells incubated in the absence (−) or in the presence (+) of 20 μM Z-VAD.fmk for different time periods. Depicted are the results obtained in one representative experiment performed in triplicates out of five independent experiments in which similar results were obtained. (C and D) Dead cell number estimation by trypan blue exclusion test in controls (C) and cells treated for the indicated time periods by EGF (E) or staurosporine (S) either in the absence (−) or in the presence (+) of Z-VAD.fmk in the same experimental conditions as described above. (E) Dead cell number as determined by trypan blue exclusion test in cells treated for 48 h by 1 nM EGF or 5 μM staurosporine (STS) either in the absence (−) or in the presence (+) of 50 μM BOC.fmk. (F) Quantification of EGF-induced cell death in p35-transiently transfected cells. GH4C1 cells were transfected with pBabe-p35 expression construct (+p35) or empty vector (−p35). Three different quantities (0.25, 0.5, and 1 μg/well) of p35 plasmid or empty vector were systematically transfected. The transfection with the highest cDNA quantity tested was cytotoxique by itself (our unpublished data). Cells transfected with 0.25 and 0.5 μg cDNA/well of either empty vector or p35 construct displayed a similar cell death for both cDNA quantities tested. Only the results obtained for transfection of 0.5 μg cDNA/well are therefore shown for better visibility. For this cDNA quantity and for the 2:1 charge ratio of TransFast to DNA, 74% of cells were transfected as determined by quantification of X-GAL coloration after a parallel cell transfection with βGAL construct inserted into pCEP (Stratagene, La Jolla, CA) vector. 48 h after transfection cells were left untreated (con) or treated with either 1 nM EGF or 5 μM STS for additional 48 h. Cell death was then analyzed by using trypan blue exclusion test. ***$p < 0.001$ for treated versus respective control groups studied in (B–F). (G) ApoDNA1 assessment of DNA fragmentation in GH4C1 cells treated for 48 h with 1 nM EGF (lane 1) alone or in combination with either 20 μM Z-VAD.fmk (lane 2) or 50 μM BOC.fmk (lane 3). The size of DNA fragments (in base pairs) is given by the lane M.

the simultaneous detection of mitochondria with MitoTracker CMXRos indicated a coincidence between AIF and MitoTracker CMXRos (yellow fluorescence resulting form the overlap of green and red light) in control cells (Figure 5C). In peroxide (100 μM; 3 h)-treated cells, used as a positive control (Djavaheri-Mergny *et al.*, 2003), and a subpopulation of EGF-treated cells, mitochondrial staining was punctate and similar to the staining observed in control cells (Figure 5C). However, in a subpopulation of EGF-treated cells punctuate AIF staining was observed despite the loss of MitoTracker CMXRos staining. In contrast to peroxide-treated cells, no nuclear translocation of AIF was seen in either subpopulation of EGF-treated cells (Figure 5C).

Together, these data showed that EGF-induced PCD in GH4C1 cells does not involve the release of cytochrome *c* and AIF from mitochondria.

Ultrastructural Morphology of EGF-induced PCD

The fact that the nuclear morphology is currently the sole criterion allowing the accurate definition of PCD pathways (Jaattela and Tschopp, 2003) prompted us to perform an ultrastructural study. The electron microscopic analysis pointed to remarkable differences in nuclear and cytoplasmic ultrastructures between control and EGF-treated cells (Figure 6A vs. B–D). In control cells, nuclei displayed a relatively uniform chromatin structure, mitochondria were clearly distinguishable, and both nuclear and plasma membranes were well preserved (Figure 6A). The addition of EGF induced the appearance of chromatin clustering forming the loose speckles (Figure 6, B–D). Twelve hours after EGF addition, mitochondria were still distinguishable in the cytoplasm (Figure 6, B and C); hence, dissolution of nucleoli occurred and small- to medium-sized cytoplasmic vacuoles occurred (Figure 6B). Some of these vacuoles were enwrapped by a double-membrane contained cytoplasmic material and were morphologically similar to autophagic vacuoles described previously in GH4C1 cells (Waguri *et al.*, 1999). At the later stage (24–48 h after EGF addition), the progression of cell death process was accompanied with further cytoplasmic vacuolation, and huge vacuoles with distinct morphology were frequently seen (Figure 6, D and E). A fraction of these vacuoles were irregular in shape, devoid of content (Figure 6E) and were very similar to those recently described in cells engaged to paraptosis (Sperandio *et al.*, 2000). In some cells, these vacuoles were so large that the cytoplasm seemed dramatically reduced and the nucleus was deformed and occupied a peripheral position (Figure 6E). The plasma membrane, however, remained well preserved (Figure 6E).

The ultrastructural analysis of GH4C1 cells treated with staurosporine showed a strikingly different, apoptosis-like

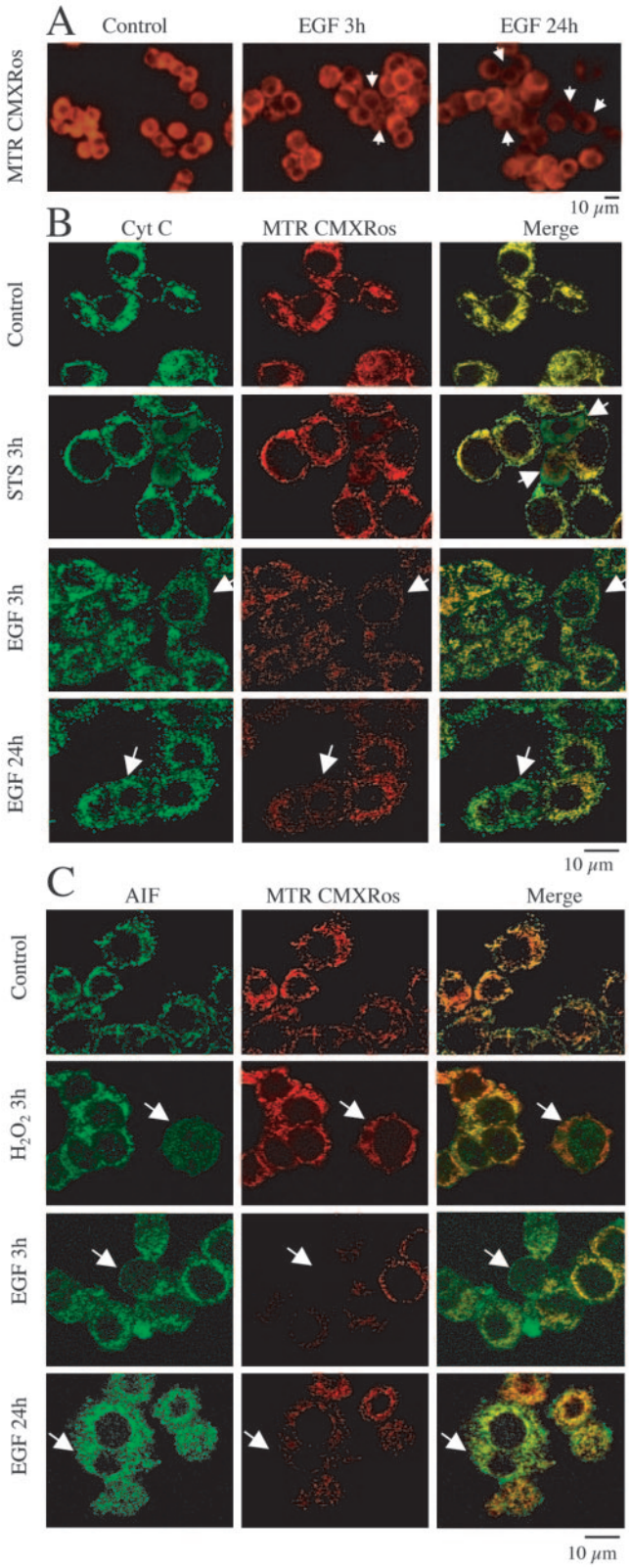

Figure 5. EGF-induced PCD in GH4C1 does not involve classical proapoptogenic mitochondrial mediators. (A) Mitochondria were visualized by staining with MitoTracker red (CMXRos). Arrows show loss of mitochondrial transmembrane potential after EGF treatment. (B) Subcellular localization of cytochrome *c* was visualized after confocal microscopy in untreated cells and cells treated with 5 μM staurosporine (STS) for 3 h or with 1 nM EGF for 3 and 24 h. Left, cytochrome *c* labeling pattern. Middle, mitochondria were visualized by staining with MitoTracker red (CMXRos). Right, overlay of both images. Images were obtained by confocal analysis of 0.2-μm optical section and are representative of four experiments. Arrows point to cytochrome *c* delocalization. (C) Same conditions as in B, excepted that peroxide (H_2O_2; 100 μM) was used as a positive control instead of staurosporine and that the primary antibody was directed against AIF. Arrows point to nuclear localization of AIF. Images are representative of four experiments. Bars, 10 μm.

morphology (Figure 6, F–H). Thus, 12 h after staurosporine addition, crescentic caps formed of aggregated chromatin abutting on nuclear envelope (Figure 6F) were seen. Later (24 and 48 h after), chromatin was more compacted and formed geometric figures (Figure 6, G and H). Moderate (Figure 6G) to severe (Figure 6H) cytoplasmic vacuolation was also observed, and at least at late stages, some of vacuoles were apparently autophagic (Kim and Klionsky, 2000). However, our efforts to confirm the autophagic nature of these vacuoles by using a relatively specific inhibitor of autophagy such as 3-methyladenine (Tolkovsky *et al*., 2002) remained unconclusive. Indeed, although used in lower concentrations than that (i.e., 20 mM) classically used (Jaattela and Tschopp, 2003), in our hands this drug was cytotoxic by itself in all concentrations (0.1–10 mM) tested (Fombonne, Reix, and Krantic, our unpublished data).

Together, the observed morphological changes further suggested that EGF triggers an original form of PCD in GH4C1 cells. To assess the relationship between this PCD and prodifferentiation effects of EGF, we studied the consequence of blocking cell death by transient overexpression of Bcl-2 on EGF-induced PRL secretion. As expected, Bcl-2 overexpression prevented the cell death induced by either staurosporine or EGF (Figure 7A). Interestingly, in Bcl-2-transfected cells the EGF-induced increase in PRL secretion was almost completely blocked (Figure 7B). This inability of transfected cells to respond to EGF by an increase in PRL secretion does not seem like a side effect of transfection because it was not seen in p35-transfected cells where EGF was still able to trigger a significant increase in PRL secretion (Figure 7, B and C).

DISCUSSION

The present report is the first to show the ability of EGF to trigger an original form of cell death through caspase-independent pathway. In addition, this cell death is apparently independent of the classical proapoptogenic mitochondrial factors such as cytochrome *c* and AIF. However, given that EGF consistently induced a loss of mitochondrial membrane potential at least in a subpopulation of GH4C1 cells, the possibility that a yet undiscovered mitochondrial mediator might trigger cell death cannot be excluded. Alternatively, the observed EGF-induced cell death might represent the first example of the hypothetical nonmitochondrial, caspase-independent cell death (Borner, 2003). The EGF-induced cell death in our model fulfils the criteria for PCD because it is an active process depending on the signaling events in dying cells (Jaattela and Tschopp, 2003). Indeed, the observed EGF-induced death is efficiently blocked through pharmacological knock-down of EGFR by its selective antagonist PKI166. In addition to the unique biochemical characteristics, EGF-induced PCD is morphologically distinct from the known forms of PCD. Thus, EGF-induced pituitary cell death displays the features intermediate to caspase-independent ap-

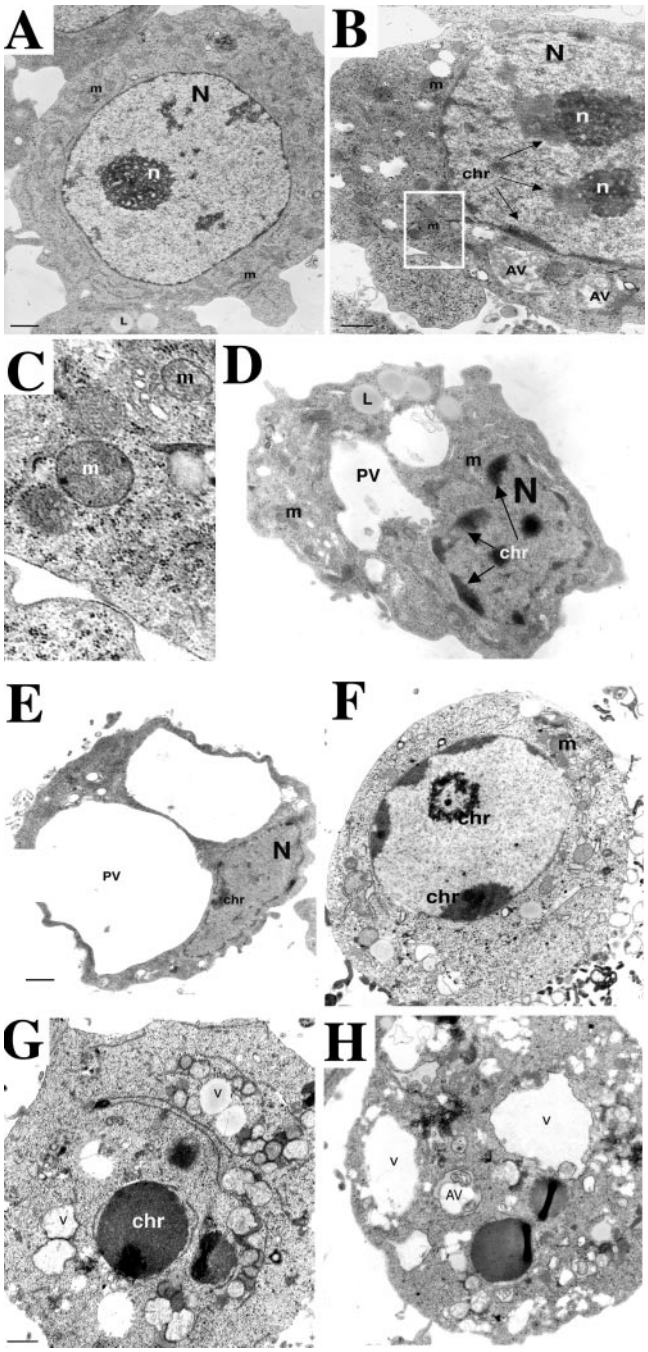

Figure 6. Incidence of EGF treatment on the ultrastructure of GH4C1 cells. (A) Control cells. (B) EGF-treated cells (12 h) characterized by nuclear chromatin condensation and the presence of autophagic vacuoles. (C) Enlargement of the inset shown in B. (D) EGF-treated cells (24 h) showing nuclei with marked patches or foci of dense chromatin. These nuclear alterations are associated with the occurrence of cytoplasmic vacuoles. (E) EGF-treated cells (48 h) displaying the enormous cytoplasmic vacuoles with morphology similar to that seen in paraptosis. (F) Staurosporine-treated cells (12 h) with dense chromatin forming the crescentic caps typical of apoptosis. (G) Staurosporine-treated cells (24 h) displaying fragmented nucleus with compacted chromatin and moderate cytoplasmic vacuolation. (H) Staurosporine-treated cells (24 h) with prominent cytoplasmic vacuolation. N, nucleus; n, nucleolus; m, mitochondria; chr, chromatin; V, vacuole; AV, autophagic vacuole; PV, paraptotic vacuole; L, lysosome. Bars, 1 μm.

optosis (presence of type 1 chromatin condensation), autophagic cell death (presence of autophagic vacuoles) and necrosis-like PCD (dissolution of nucleoli and presence of large-sized vacuoles) (Jaattela and Tschopp, 2003).

The characterized EGF-mediated cell death in GH4C1 cells is insensitive to caspase inhibitors and according to this particular criterion it might be apoptotic, autophagic, or necrotic in nature. Indeed, it has been proposed that even in classical, caspase-dependent apoptosis some morphological characteristics (e.g., cytoplasmic events) display caspase independence. According to that hypothesis, only nuclear events are caspase dependent (Borner and Monney, 1999). However, the insensitivity of DNA fragmentation to broad-range caspase inhibitors in our assay strongly argues against the involvement of classical apoptosis in EGF-induced cell death. Moreover, EGF is unlikely to induce necrosis in GH4C1 cells because the integrity of plasma membrane is well preserved in EGF-treated cells as shown by our electron microscopy data. Conversely, EGF-induced PCD has some morphological characteristics of autophagy because double-membrane wrapped vacuoles filled with cytoplasmic content were seen in EGF-treated cells. The presence of autophagic vacuoles in GH4C1 cells dying by staurosporine-induced apoptosis points to the fact that autophagy might occur secondary to cell death induction irrespectively of the nature of the cell death trigger (staurosporine or EGF) and death modality (classical apoptosis or EGF-specific PCD). Nevertheless, the concomitant appearance of autophagic vacuoles and chromatin alterations as early as 12 h after EGF addition argues strongly against that possibility and rather suggests that autophagic component represents an intrinsic part of the original, heterogeneous phenotypic expression of EGF-induced PCD. Indeed, in pure autophagic phenotype cytoplasm is actively destroyed through extensive vacuolization long before the chromatin changes become apparent (Lockshin and Zakeri, 2002).

In agreement with our conclusions on the heterogeneous phenotype of the observed caspase-independent PCD, EGF also induced the appearance of huge cytoplasmic vacuoles of irregular shape reminiscent of those seen in cells dying without DNA cleavage by paraptosis (Sperandio *et al.*, 2000). Moreover, these "paraptosis-like"-EGF–induced vacuoles were clearly distinct from autophagic vacuoles because they were much greater and devoid of intracellular content. Finally, according to the type 1 of chromatin condensation observed here, EGF-induced PCD might be classified as caspase-independent apoptosis similar to that previously described in T lymphocytes (Dumont *et al.*, 2000; Bidère and Senik, 2001). However, this possibility also seems unlikely because 1) the pattern of DNA fragmentation seen in GH4C1 cells corresponds to the profile seen in classical, caspase-dependent apoptosis rather than to large-scale fragmentation characteristic for caspase-independent apoptosis; and 2) EGF is inefficient in triggering the translocation of the known mediator of caspase-independent apoptosis such as AIF from GH4C1 cell mitochondria to nucleus.

In line with the failure of mitochondrial AIF efflux upon EGF, the absence of EGF-induced cytochrome *c* release from mitochondria shown here provides the additional evidence for the absence of the classical mitochondrial factors involvement in EGF-induced PCD of GH4C1 cells. Neither of these two proapoptogenic factors was therefore liberated from mitochondria despite the loss of $\Delta\varphi_m$ in agreement with the reported lack of direct causal relationship between cell death and loss of $\Delta\varphi_m$ (Minamikawa *et al.*, 1999; Jaattela and Tschopp, 2003).

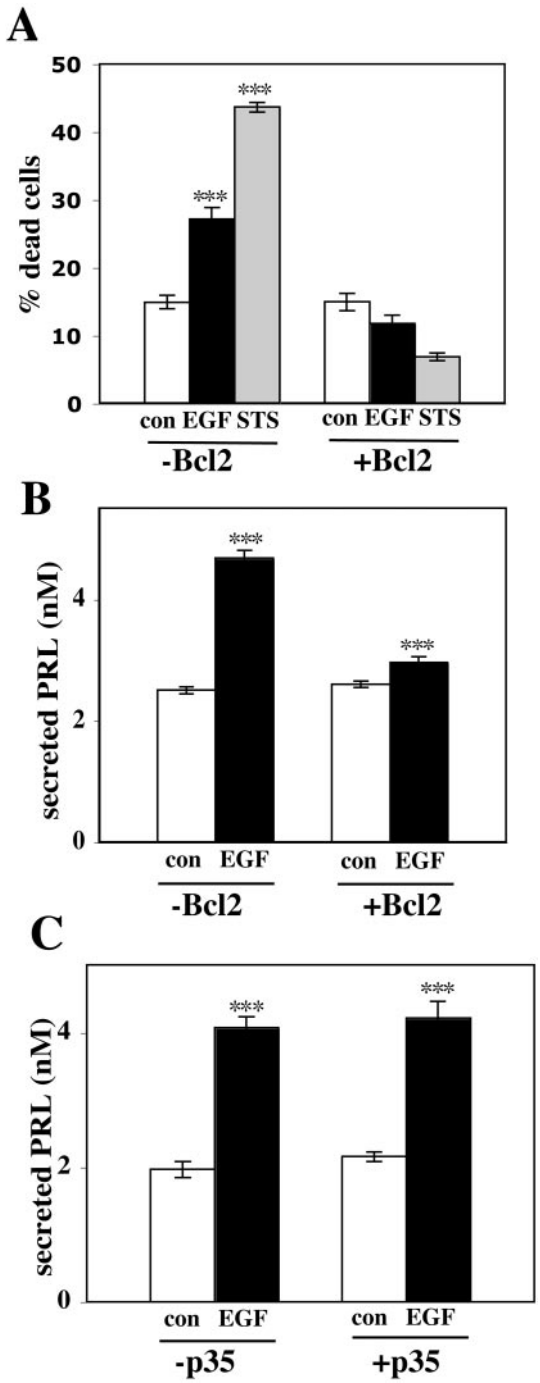

Figure 7. Bcl-2 overexpression in GH4C1 cells blocks EGF-induced cell death and EGF-induced PRL secretion. (A) Quantification of EGF-induced cell death in Bcl-2–transfected cells. GH4C1 cells were transfected with pcDNA-Bcl-2 expression construct (+Bcl-2) or empty vector (−Bcl-2) as described in the legend of the Figure 4 for p35 transfections. ***$p < 0.001$ for EGF- and staurosporine (STS) treated versus control (con) cells in (−Bcl-2) group. (B and C) PRL secretion by Bcl-2 (B) or p35 (C) transiently transfected GH4C1 cells. Forty-eight hours after transfection cells were treated or not for additional 48 h by EGF (1 nM). ***$p < 0.001$ for EGF-treated versus control cells.

Besides, our study suggests an original relationship existing between the execution of different genetic programs such as differentiation, cell division, and death because the inhibition of the EGF-induced PCD blocks the differentiation-like actions of EGF. Indeed, in our experimental conditions, the overexpression of Bcl-2 was sufficient to protect GH4C1 cells from EGF-induced cell death in agreement with its capacity to prevent caspase-dependent and -independent apoptosis (Borner, 2003) as well as necrosis (Proskuryakov *et al*., 2003). However, Bcl-2 overexpression could not induce the increase in PRL secretion in the absence of EGF in contrast to what would be expected if EGF-induced differentiation of GH4C1 cells was a "default" program such as proposed for some other differentiation factors (Gao and Zelenka, 1997; Dolznig *et al*., 2002).

Another important observation coming from our Bcl-2 overexpression assays is the suppression of EGF capacity to increase PRL secretion in transfected cells. This is not a nonspecific consequence of transfection because EGF increases PRL secretion in p35-transfected cells with an equal efficiency as in mock-transfected cells. The reasons for the inefficiency of EGF in induction of PRL secretion in Bcl-2–transfected cells remain unknown. It is however tempting to speculate that they might be related to survival-independent actions of Bcl-2 such as, for example, its interaction with integral proteins of endoplasmic reticulum (Ng *et al*., 1997; Ng and Shore, 1998) that might impinge on hormone secretions. In terms of the relationship between the programmed cell death and differentiation, our results suggest that differentiation might be blocked in the absence of cell death. Given the fact that Bcl-2 might have influenced by itself the differentiation marker studied (PRL secretion), the use of Bcl-2 to block cell death could introduce a bias to this interpretation. However, it seems from our data that if any, such a bias would concern only EGF-stimulated conditions because there is no difference in basal PRL secretion between Bcl-2–transfected and nontransfected cells (Figure 7B). The definitive clarification of this particular point should thus await a development of another universal cell death inhibitor without potential actions on endoplasmic reticulum. With this caution in mind, our data nevertheless raise the possibility that the successful differentiation of a given subpopulation of cells requires a programmed death of another part of the same cell population. In this hypothesis, two possible mechanisms could be involved: either a subpopulation of cells should die to ensure the optimal availability of trophic factors to remaining cells to allow their survival and differentiation or dying cells might produce a competent factor necessary for triggering differentiation of surviving cells.

Together, our data bring further evidence for the panoply of phenotypic expressions of PCD and suggest that the various modes of known death programs expression may coincide in a single cell, conferring a heterogeneous phenotype to these PCDs (Wyllie and Golstein, 2001). Moreover, based on our biochemical, pharmacological, and morphological data, it seems reasonable to assume that the mechanisms underlying these original caspase- and known pro-apoptogenic mitochondria effector-independent PCDs involve the combinatorial engagement of cell death effectors previously discovered in discrete death pathways (apoptosis, autophagy, and necrosis). Such combinatorial engagement might be in the origin of heterogeneous morphological expression of the related death outcome. In addition, such PCD characterized by heterogeneous phenotype might be causally associated to differentiation as shown here for EGF-induced PCD linked to the differentiation of pituitary lactotropes from somato-lactotrope precursors.

In conclusion, our data suggest that differentiation-linked PCDs might differ from other forms of PCDs in terms of

their heterogeneous phenotype and evolutionary conservation. Indeed, some (i.e., caspase-independence and morphological expression) but not all (proapoptogenic mitochondrial factors involvement) molecular characteristics of the EGF-induced PCD in pituitary cells are very similar to those reported in PCD observed during the differentiation of the unicellular organism *Dictyostelium discoideum* (Cornillon *et al.*, 1994; Arnoult *et al.*, 2001). In this light, the EGF-induced differentiation and PCD characterized here in the pituitary GH4C1 cell model seem as a valuable tool for the study of the integrating mechanism(s) involved in the new types of PCD in mammalian cells and their relationship to other genetic programs. Better understanding of these phenomena might have large implications in both fundamental and applied fields of development and carcinogenesis.

ACKNOWLEDGMENTS

We are greatly indebted to Drs. A. Matter (Novartis AG) for a kind gift of PKI166, P. Mellon (University of California, San Diego), and D. Weiner (University of California, San Francisco) for the gift of LβT2 cell line. We also thank Drs. C. Susini and J. Daillie for constructive discussions and helpful suggestions and I. Goddard for the critical reading of the manuscript. This work was supported by Ligue contre le Cancer, Fondation Schlumberger, and the National Institutes of Health (to P.M.), Ligue contre le Cancer (to A.E.) and Foundation pour la Recmerche Medicale (to J.F.).

REFERENCES

Aanestad, M., Rotnes, J., Torjesen, P., Haug, E., Sand, O., and Bjoro, T. (1993). Epidermal growth factor stimulates the prolactin synthesis and secretion in rat pituitary cells in culture (GH4C1 cells) by increasing the intracellular concentration of free calcium. Acta Endocrinol. *128*, 361–366.

Arnoult, D., Gaume, B., Karbowski, M., Sharpe, J., Cecconi, F., and Youle, R. (2003). Mitochondrial release of AIF and EndoG requires caspase activation downstream of Bax/Bak-mediated permeabilization. EMBO J. *22*, 4385–4399.

Arnoult, D., *et al*. (2001). On the evolutionary conservation of the cell death pathway: mitochondrial release of an apoptosis-inducing factor during *Dictyostelium discoideum* cell death. Mol. Biol. Cell *12*, 3016–3030.

Bidère, N., and Senik, A. (2001). Caspase-independent apoptotic pathways in T lymphocytes: a minireview. Apoptosis *6*, 371–375.

Birman, P., Michard, M., Li, J., Peillon, F., and Bression, D. (1987). Epidermal growth factor-binding sites, present in normal human and rat pituitaries, are absent in human pituitary adenomas. J. Clin. Endocrinol. Metab. *65*, 275–281.

Bogdan, S., and Klambt, C. (2001). Epidermal growth factor receptor signaling. Curr. Biol. *11*, R292–R295.

Borner, C. (2003). The bcl-2 protein family: sensors and checkpoints for life-or-death decisions. Mol. Immunol. *39*, 615–647.

Borner, C., and Monney, L. (1999). Apoptosis without caspases: an inefficient molecular guillotine? Cell Death Differ. *6*, 497–507.

Budihardjo, I., Oliver, H., Lutter, M., Luo, X., and Wang, X. (1999). Biochemical pathways of caspase activation during apoptosis. Annu. Rev. Cell Dev. Biol. *15*, 269–290.

Cornillon, S., Foa, C., Davoust, J., Buonavista, N., Gross, J., and Golstein, P. (1994). Programmed cell death in *Dictyostelium*. J. Cell Sci. *107*, 2691–2704.

Danielsen, A., and Maihle, N. (2002). The EGF/ErbB receptor family and apoptosis. Growth Factors *20*, 1–15.

Djavaheri-Mergny, M., Wietzerbin, J., and Besancon, F. (2003). 2-methoxyestradiol induces apoptosis in Ewing sarcoma cells through mitochondrial hydrogen peroxide production. Oncogene *22*, 2558–2567.

Dolznig, H., Habermann, B., Moriggl, R., Beug, H., and Mullner, E. (2002). Apoptosis protection by the Epo target Bcl-XL allows factor independent differentiation of primary erytroblasts. Curr. Biol. *12*, 1076–1085.

Dumont, C., Dürrbach, A., Bidère, N., Rouleau, M., Kroemer, G., Bernard, G., Hirsch, F., Charpentier, B., Susin, S., and Senik, A. (2000). Caspase-independent commitment phase to apoptosis in activated blood T lymphocytes: reversibility at low apoptotic insult. Blood *96*, 1030–1038.

Epelbaum, J., Enjalbert, A., Krantic, S., Musset, F., Bertrand, P., Rasolonjanahary, R., Shu, C., and Kordon, C. (1987). Somatostatin receptors on pituitary somatotrophs, thyrotrophs and lactotrophs: pharmacological evidence for loose coupling to adenylate cyclase. Endocrinology *121*, 2177–2185.

Felix, R., Meza, U., and Cota, G. (1995). Induction of classical lactotropes by Epidermal growth factor in rat pituitary cell cultures. Endocrinology *136*, 939–946.

Forcet, C., Ye, X., Granger, L., Corset, V., Shin, H., Bredesen, D., and Mehlen, P. (2001). The dependence receptor DCC (deleted in colorectal cancer) defines an alternative mechanism for caspase activation. Proc. Natl. Acad. Sci. USA *98*, 3416–3421.

Gao, C., and Zelenka, P. (1997). Cyclins, cyclin-dependent kinases and differentiation. Bioessays *19*, 307–315.

Golstein, P., Aubry, L., and Levraud, J.-P. (2003). Cell-death alternative model organisms: why and which? Nat. Rev. Mol. Cell. Biol. *4*, 1–10.

Hockenbery, D., Oltvai, Z., Yin, X., Milliman, C., and Korsmeyer, S. (1993). Bcl-2 functions in an anti-oxidant pathway to prevent apoptosis. Cell *75*, 241–251.

Huff, K., and Guroff, G. (1981). Nerve growth factor induced alteration in the response of PC12 pheochromocytoma cells to epidermal growth factor. J C ell Biol. *88*, 189–198.

Jaattela, M., and Tschopp, J. (2003). Caspase-independent cell death in T lymphocytes. Nat. Immunol. *4*, 416–423.

Johnson, L., Baxter, J., Vlodavsky, I., and Gospodarowitz, D. (1980). Epidermal growth factor and expression of specific genes: effects on cultured rat pituitary cells are dissociable from the mitogenic response. Proc. Natl. Acad. Sci. *77*, 394–398.

Kanasaki, H., Fukunaga, K., Takahashi, K., Miyazaki, K., and Miyamoto, E. (2000). Involvement of p38 mitogen-activated protein kinase activation in bromocriptine-induced apoptosis in rat pituitary GH3 cells. Biol. Reprod. *62*, 1486–1494.

Kim, J., and Klionsky, D. (2000). Autophagy, cytoplasm-to-vacuole targeting pathway and pexophagy in yeast and mammalian cells. Annu. Rev. Biochem. *69*, 303–342.

Kineman, R., and Frawley, L. (1994). Secretory characteristics and phenotypic plasticity of growth hormone and prolactin-producing cell lines. J. Endocrinol. *140*, 455–463.

Leu, C., Chang, C., and Hu, C. (2000). Epidermal growth factor (EGF) suppresses staurosporine-induced apoptosis by inducing mcl-1 via the mitogen-activated protein kinase pathway. Oncogene *19*, 1665–1675.

Liu, F., Austin, D., Mellon, P., Olefsky, J., and Webster, N. (2002a). GnRH activates ERK1/2 leading to the induction of c-fos and LH-beta protein expression in L-betaT2cells. Mol. Endocrinol. *16*, 419–434.

Liu, J., Baker, R., Sun, C., Sundmark, V., and Elsholtz, H. (2002b). Activation of G0-coupled dopamine D2 receptors inhibits ERK1/ERK2 in pituitary cells. J. Biol. Chem. *39*, 35819–35825.

Lockshin, R., and Zakeri, Z. (2002). Caspase-independent cell deaths. Curr. Opin. Cell Biol. *14*, 727–733.

Mellinghoff, I., Tran, C., and Sawyers, C. (2002). Growth inhibitory effects of the dual ErbB1/ErbB2 tyrosine kinase inhibitor PKI-166 on human prostate cancer xenografts. Cancer Res. *62*, 5254–5259.

Minamikawa, T., Williams, D., Bowser, D., and Nagley, P. (1999). Mitochondrial permeability transition and swelling can occur reversibly without inducing cell death in intact human cells. Exp. Cell Res. *246*, 26–37.

Nagata, S. (1997). Apoptosis by death factor. Cell *88*, 355–365.

Ng, F., Nguyen, M., Kwan, T., Branton, P., Nicholson, D., and Cromlish, J. (1997). p28 Bap31, a Bcl-2/Bcl-XL- and procaspase-8-associated protein in the endoplasmic reticulum. J. Cell Biol. *139*, 327–338.

Ng, F., and Shore, G. (1998). Bcl-XL cooperatively associates with the Bap31 complex in the endoplasmic reticulum, dependent on procaspase-8 and Ced-4 adaptor. J. Biol. Chem. *273*, 3140–3143.

Partanen, A. (1990). Epidermal growth factor and Transforming growth factor-alpha in the development of epithelial-mesenchymal organs of the mouse. Curr. Top. Dev. Biol. *24*, 31–55.

Peles, E., and Yarden, Y. (1993). Neu and its ligands: from an oncogene to neural factors. Bioessays *15*, 815–824.

Proskuryakov, S., Konoplyannikov, A., and Gabai, V. (2003). Necrosis: a specific form of programmed cell death. Exp. Cell Res. *283*, 1–16.

Ramsdell, J. (1991). Voltage-dependent calcium channels regulate GH4 pituitary cell proliferation at two stages of the cell cycle. J. Cell Physiol. *146*, 197–206.

Rao, R., Hermel, E., Castro-Obregon, S., del Rio, G., Ellerby, L., Ellerby, H., and Bredesen, D. (2001). Coupling endoplasmic reticulum stress to the cell death program (mechanism of caspase activation). J. Biol. Chem. *276*, 33869–33874.

Schonbrunn, A., Krasnoff, M., Westendorf, J., and Tashijan, J.A. (1980). Epidermal growth factor and thyrotropin-releasing hormone act similarly on a clonal pituitary cell line. J. Cell Biol. *85*, 786–797.

Sloviter, R. (2002). Apoptosis: a guide for perplexed. Trends Pharmacol. Sci. *23*, 19–24.

Sperandio, S., de Belle, I., and Bredesen, D. (2000). An alternative, nonapoptotic form of programmed cell death. Proc. Natl. Acad. Sci. *97*, 14 376–314 381.

Tolkovsky, A., Xue, L., Fletcher, G., and Borutaite, V. (2002). Mitochondrial disappearance from cells: a clue to the role of autophagy in programmed cell death and disease? Biochimie *84*, 233–240.

Waguri, S., Kohmura, M., Gotow, T., Watanabe, T., Ohsawa, Y., Kominami, E., and Uchiyama, Y. (1999). The induction of autophagic vacuoles and the unique endocytic compartments, C-shaped multivesicular bodies, in GH4C1 cells after treatment with 17-beta estradiol, insulin and EGF. Arch. Histol. Cytol. *62*, 423–434.

Weiss, S., Reynolds, B., Vescovi, A., Morshead, C., Craig, C., and van Der Kooy, D. (1996). Is there a neural stem cell in the mammalian forbrain? Trends Neurosci. *19*, 387–393.

Wyllie, A., and Golstein, P. (2001). More than one way to go. Proc. Natl. Acad. Sci. *98*, 11–13.

Yoshinaga, N., Murayama, T., and Nomura, Y. (1998). Death by a dopaminergic neurotoxin, 1-methyl-4-phenylpyridinium ion (MPP+) and protection by EGF in GH3 cells. Brain Res. *794*, 137–142.